What Can Catchment Transit Time Distributions Tell Us About Runoff Mechanisms? Exploring "Age Equifinality" with an Integrated Surface-Groundwater Model.

Daniel Wilusz[1*], Reed Maxwell[2], Anthony Buda[3], William Ball[1,4], Ciaran Harman[1]

[1]Department of Environmental Health and Engineering, The Johns Hopkins University, Baltimore, Maryland, USA.
[2] Hydrologic Science and Engineering Program, Integrated GoundWater Modeling Center, Department of Geology and Geological Engineering, Colorado School of Mines, Golden, Colorado, USA.
[3]Pasture Systems and Watershed Management Research Unit, Agricultural Research Service, USDA, University Park, Pennsylvania, USA.
[4]Chesapeake Research Consortium, Edgewater, Maryland, USA. *Contact: Dano Wilusz at dwilusz1@jhu.edu

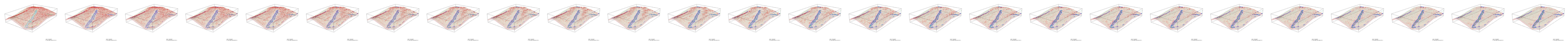

1. Abstract

Motivation

- The ability to use water age to make inferences about dominant runoff mechanisms depends on the degree of "age equifinality" in a watershed.
- "Age-equifinality" is defined here as the phenomenon where significant volumes of similarly-aged water are discharged at the same time from different runoff generation mechanisms.

Experimental objectives

- To develop better tools for simulating time-varying transit times through multiple catchment flow pathways.
- To understand the extent and mechanistic drivers of age-equifinality in a relatively complex, physically-based watershed modeling environment.

What was found (preliminary)

- Incorporating information about catchment velocities into the calibration of a physically-based model improved parameter selectivity, though less than expected.
- A simple modification to conventional particle tracking algorithms can track the age of ET.
- Substantial age-equifinality was observed, especially between overland flow, interflow, and shallow groundwater recharge.
- Post-processing of model output using rank StorAge Selection functions helps reveal mechanistic drivers.

Partial support provided by NSF CBET Water, Sustainability, and Climate Grant (ID#1360345) and a 2016 Geological Society of America Student Research Grant.

2. FD36 at Mahantango, PA USA: a USDA experimental catchment.

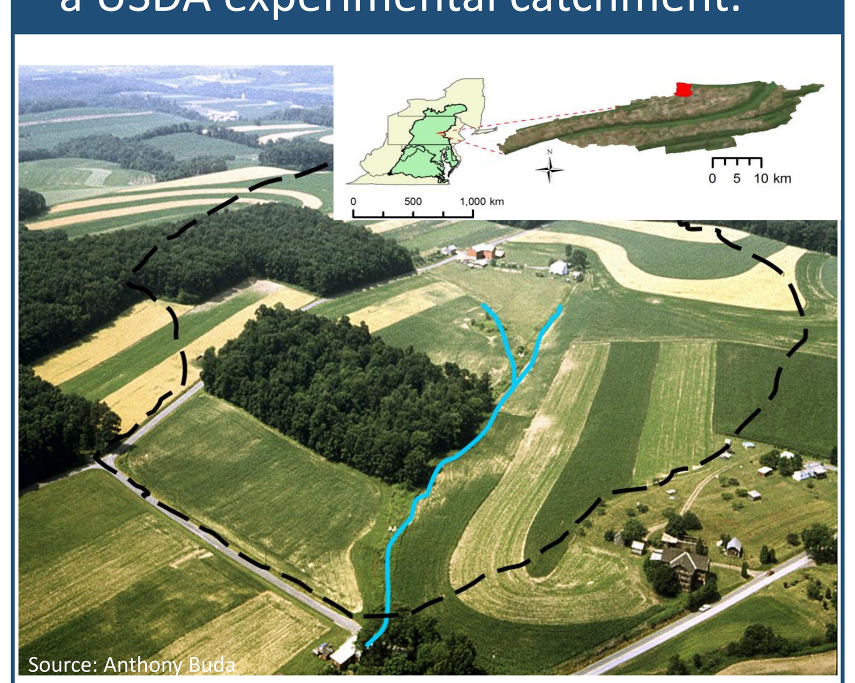

Figure 1. Photograph of the 0.4 km^2 study catchment. This study uses discharge data from the outlet, meteorological data from a nearby weather station, and various measurements of watershed properties.

3. Benchmark hydrologic model: PARFLOW

A virtual modeling testbed was constructed using the fully distributed PARFLOW (PARallel FLOW) model [1-4] with SLIM-FAST particle tracking code [5].

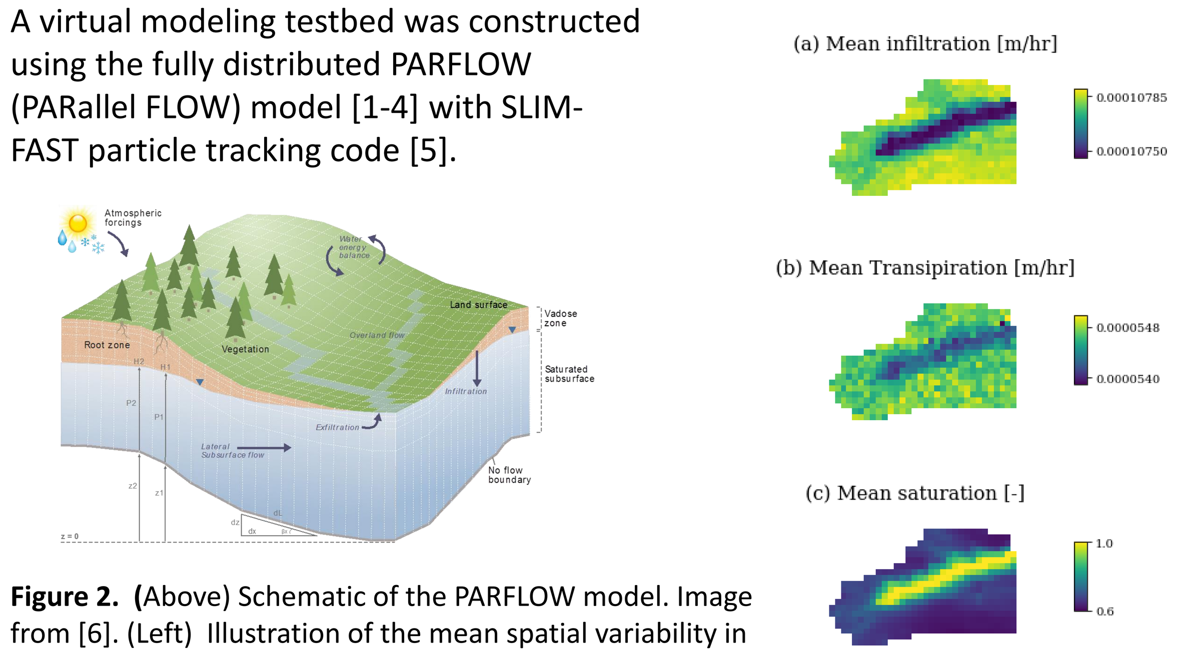

Figure 2. (Above) Schematic of the PARFLOW model. Image from [6]. (Left) Illustration of the mean spatial variability in state variables simulated by our calibrated model.

4. Novel approach to "partitioned" particle tracking

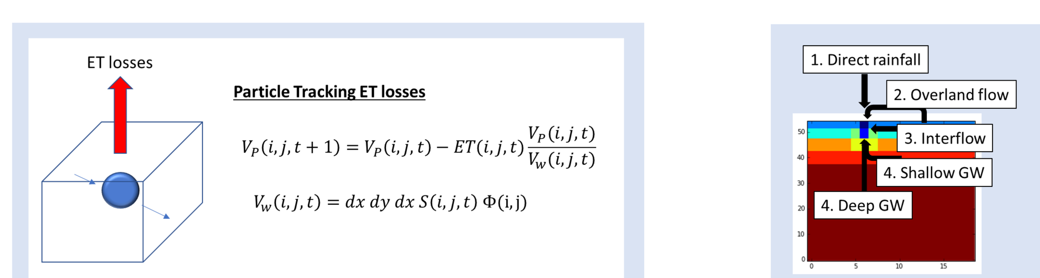

Figure 3. (Left) Algorithm used to account for particle water loss to ET in the SLIM-FAST code. (Right) Conceptual diagram showing how water particles were partitioned into five different flow pathways reaching the stream. The figure is a cross section of the model domain with the soil layer and streambed (darkest blue) on top and the fractured bedrock at the bottom.

4. GLUE calibration against celerity and velocity

Figure 4. The calibration was performed on the 2D transect shown in (a) and (b) and applied to the 3D model.

(a)

(b)

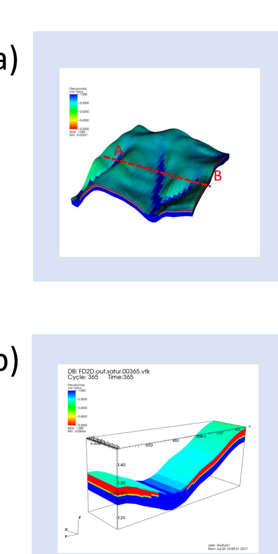

Figure 5. Sensitivity analysis performed on results from a Generalized Likelihood Uncertainty Estimation (GLUE) with 22k runs. "Behavioral" runs had a Kling-Gupta Efficiency greater than 0.5 and baseflow water age matching nearby field observations (8-10 months).

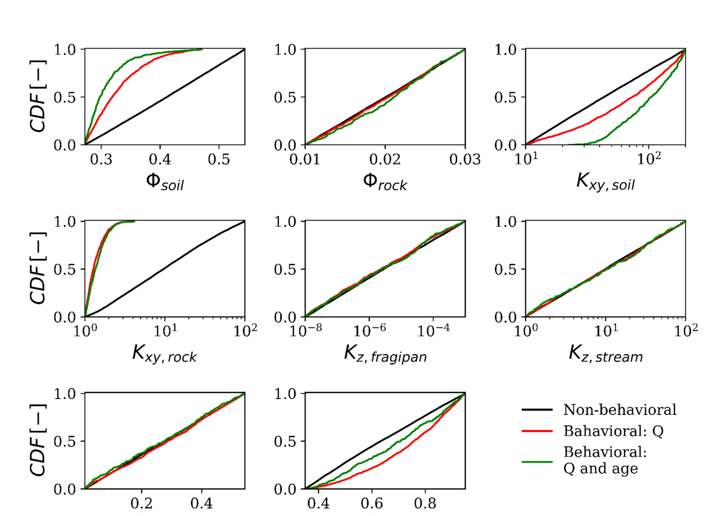

Table 1. (Right) Best performing parameters from GLUE. Bracketed values show the range considered.

Layer	Ksat [m/hr]	Ksat,xy [-]	Ksat,z [-]	Kf,z [1/m]	Porosity [-]	VG alpha [m]	VG n [-]
Streambed	0.062	1.0	37.4 [1,100]	0	0.18 [.01,.5]	2.32	1.29
Soil	0.062	35.2 [10,200]	1.0	0	0.29 [0.28, 0.53]	2.32	1.29
Fragipan	0.062	1.0	2.20E-05 [1e-8,1e-3]	0	0.29	2.32	1.29
Fractured bedrock	0.062	1.02 [1,100]	1.0	0.79 [0.35, 0.93]	0.02 [0.01, 0.03]	2.32	1.29
References	8			8	8,10	10	10

6. Time-varying transit times of five runoff mechanisms

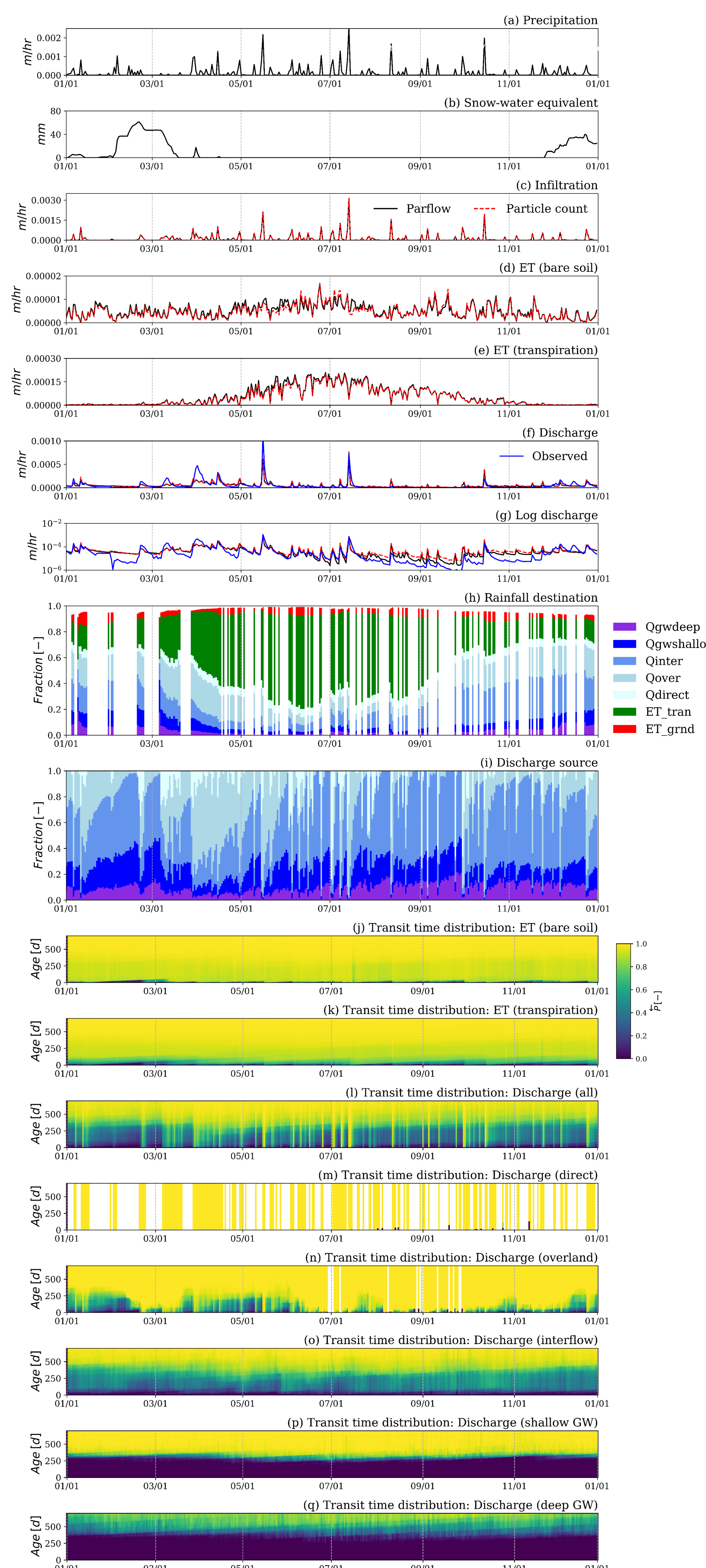

Figure 6. Time-series of model output for the year 2014. Continued in next panel.

7. Different flow pathways, same age.

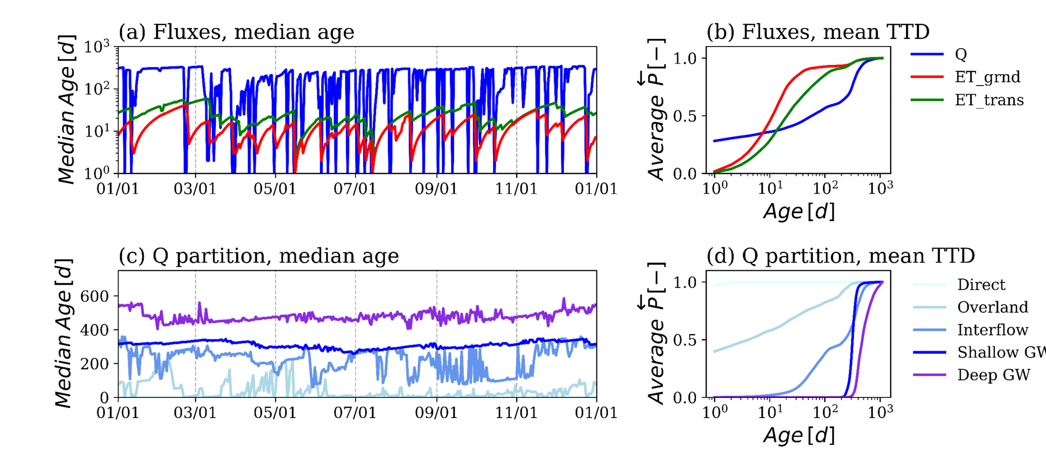

Figure 7. (Above). (a) and (c) show a time-series of the median age of water in different fluxes and different partitions of discharge. (b) and (d) show the time- and flow-averaged transit time distribution (TTD) for the entire year.

Figure 6 (con't). (Left) Plots (a-g) show the hydrologic simulation, plots (h-i) show the estimates of partitioning fraction, and plots (j-q) show the time-varying transit time simulated for each runoff mechanism.

8. rank StorAge Selection functions help reveal processes driving age variability and equifinality

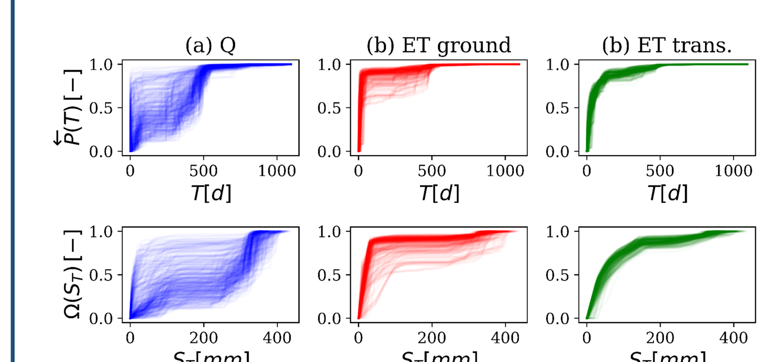

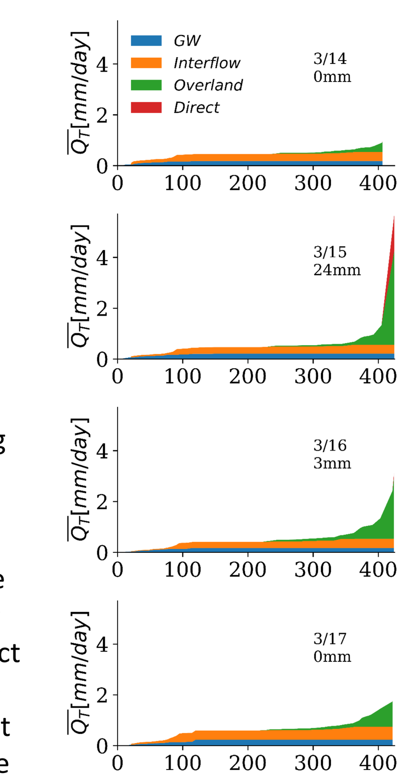

Figure 9. Plots compare the time variability of the transit time distribution (with each line representing 1 day) and the rank Storage Selection Function (described in [10]).

Figure 10. Plots of the age-ranked storage discharge complement relationship (Harman, in prep.) on four consecutive days show, for example, the role of direct rainfall and overland flow in producing the "inverse-storage effect". Larger values on the axes represent younger ranked storage (on the x-axis) and discharge (on the y-axis).

9. Limitations and future work

- The PARFLOW model was calibrated to observations of water age inferred from steady-state modeling.
- rSAS modeling (Figures 9 and 10) was done on a 2-D model run. It will be extended to 3D.
- The modeling results are being interrogated to understand exactly why interflow varies more than the other components.

References: (1) Ashby, S.; Falgout, R. A parallel multigrid preconditioned conjugate gradient algorithm for groundwater flow simulations. Nucl. Sci. Eng. 1996, 124, 145–159. **(2)** Jones, J.; Woodward, C. Newton–Krylov-multigrid solvers for large-scale, highly heterogeneous, variably saturated flow problems. Adv. Water Resour. 2001, 24, 763–774. **(3)** Kollet, S.; Maxwell, R. Integrated surface–groundwater flow modeling: A free-surface overland flow boundary condition in a parallel groundwater flow model. Adv. Water Resour. 2006, 29, 945–958. **(4)** Maxwell, R. A terrain-following grid transform and preconditioner for parallel, large-scale, integrated hydrologic modeling. Adv. Water Resour. 2013, 53, 109–117. **(7)** Maxwell, R.; Tompson, A. SLIM-FAST: a user's manual, Lawrence Livermore National Laboratory, Livermore, California. 2006. **(8)** Maxwell, R, "ParFlow Short Course", slides presented at the Beyond Groundwater Modeling short course, May 25-27, Golden, Co (2016). **(9)** W.J., G.; Folmar, G. J.; Urban, J. B. Field Data and Ground Water Modeling in a Layered Fractured Aquifer. Groundwater 1999, 37 (2), 175–184. (9) Burton, W. C.; Plummer, L. N.; Busenberg, E.; Lindsey, B. D.; Gburek, W. J. Influence of fracture anisotropy on ground water ages and chemistry, Valley and Ridge province, Pennsylvania. Ground Water 2002, 40 (3), 242–257. **(10)** Troch, P. A.; Smith, J. A.; Wood, E. F.; de Troch, F. P. Hydrologic controls of large floods in a small basin: central Appalachian case study. J. Hydrol. 1994, 156 (1–4), 285–309. . (14) Harman, C. J. Time Variable Transit Time Distributions and Transport: Theory and Application to Storage-dependent Transport of Chloride in a Watershed. Water Resour. Res. 2015, 1–30.